Magnetic Field Effects in Chemical Systems

Summary of the D.Phil. thesis by Christopher T. Rodgers[1]

1 Introduction

Magnetic fields can alter the rate, yield or product distribution of chemical reactions[2,3]. This thesis is concerned with the — relatively uninvestigated — effects of weak magnetic fields $B_0 \sim 1\,\mathrm{mT}$ found in nature. This thesis is motivated by a desire to lay firm physico-chemical foundations for discussion of the biological effects of magnetic fields. It presents new theoretical tools and applies them to interpret experimental measurements.

2 Radical Pair Mechanism

The radical pair mechanism (RPM)[4–6] provides a basis for the interpretation of magnetic field effects (MFEs). Figure 1 summarises the RPM for radicals in solution. The essential features are:

- The precursor(s) (Pre) react, e.g. via electron transfer, to form a radical pair (RP) *i.e.* two radicals (A and B) with correlated electron spins. I assume throughout that the RP is generated in a singlet state. It is trivial to adapt the results for triplet-born RPs.
- Those RPs that do not recombine immediately separate and diffuse through the solvent.
- During this diffusive excursion, the RP spin state evolves (between singlet and triplet states) under the influence of the RP spin Hamiltonian, which contains, crucially, the Zeeman interaction of the unpaired electrons with the surrounding magnetic field.
- Some RPs separate for good, forming escape products (EP).
- Other RPs move back together. Whether they react during a re-encounter depends on the spin evolution during the preceding diffusive excursion. RPs which re-encounter in a singlet state react to form the "singlet product" (SP). RPs in a triplet state form other "triplet products" (TP).

Spin evolution between singlet and triplet states during diffusive excursions is central to the RPM. Since the RPM is a kinetic effect, even weak magnetic fields, with energies far less than $k_\mathrm{B}T$, may cause significant changes in singlet yield.

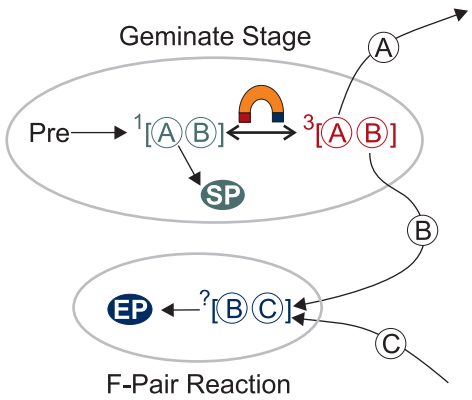

Figure 1: Radical pair mechanism in liquids.

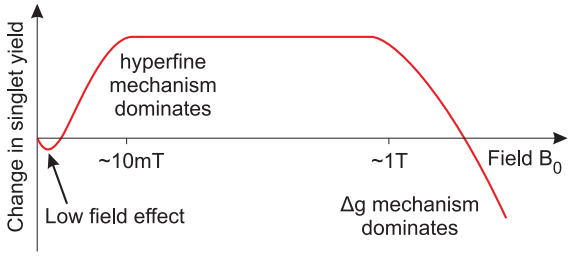

Figure 2: Typical magnetic field effects in organic RPs from zero field up to a few Tesla.

3 Time-independent magnetic fields

The simplest MFE experiment, a "MARY spectrum", measures the singlet yield Φ_S as a function of the strength of a time-independent ("static") applied magnetic field B_0. Figure 2 shows the behaviour that is expected.

According to the RPM, the singlet yield is approximated by

$$\Phi_S = \int_0^\infty \left\langle \hat{P}^S \right\rangle (t) f(t)\, \mathrm{d}t \tag{1}$$

where $\left\langle \hat{P}^S \right\rangle (t)$ is the probability that the RP will be in a singlet state at time t and $f(t)$ is the probability that the radicals will first re-encounter at time t.

3.1 Empirical re-encounter probability

The correct form for $f(t)$ has long been uncertain. The most popular choices are the "exponential model"[7]

$$f(t) = k\mathrm{e}^{-kt} \tag{2}$$

or the "diffusion model"[8–10]

$$f(t) = at^{-3/2} \exp\left(-b/t\right) \tag{3}$$

where a, b and k are constants.

I developed a method to extract an empirical $f(t)$ from MFE data[11]. For each field where the singlet yield has been measured, it uses a novel algorithm to calculate the singlet probability $\left\langle \hat{P}^S \right\rangle (t)$ before solving equation (1) for $f(t)$. Introducing appropriate Tikhonov and Maximum Entropy regularisation methods and using experimental data from the reaction of isotopomers of pyrene and N,N-dimethylaniline made it possible to solve this highly ill-posed problem. The results are given in Figure 3. Surprisingly, this analysis demonstrates that the simple exponential model is closest to experiment.

3.2 Characterising MARY spectra

MARY spectra for RPs in solution may be characterised by a small number of parameters (see Figure 4). I derived "rules of thumb" to predict trends in these parameters. In particular, I assessed when there would be a strong low field effect (LFE). LFEs are extremely important in the debate on the health effects of EMFs and on the magnetic sense of birds. Nevertheless, the literature contained apparently contradictory statements arising from X-ray irradiation studies[12,13] and from perturbation theory[14].

I developed a Monte Carlo approach to tackle this problem. Significantly, I found that the necessary "rules of thumb" differ markedly when the ongoing RP reactions are slower than, comparable to or faster than the effective hyperfine couplings in the RP. It seems likely that this accounts for the apparent disagreement in the literature.

I also investigated a commonly used semiclassical approximation[15] for RP spin evolution, shedding fresh light on its physical basis. Unfortunately, at low fields this approximation was shown to be qualitatively incorrect and ought no longer to be used.

4 Time-dependent magnetic fields

I investigated the combined effects of radiofrequency and weak static magnetic fields[16–18]. Figure 5 plots the effect of relative orientation θ of these fields[16,17] showing the breakdown of normal EPR selection rules. This experiment would be diagnostic for RPM involvement in biology.

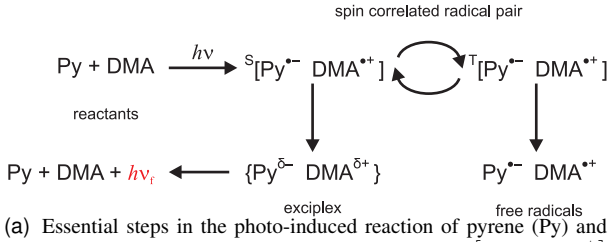

(a) Essential steps in the photo-induced reaction of pyrene (Py) and N,N-dimethylaniline (DMA) via the radical pair state $[Py^{\bullet-}\ DMA^{\bullet+}]$ which is responsible for the magnetic field-sensitivity of the exciplex fluorescence. $h\nu$ signifies the incoming ultraviolet radiation and $h\nu_f$ the observed exciplex fluorescence.

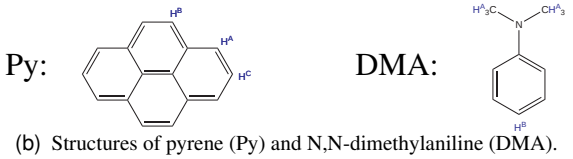

(b) Structures of pyrene (Py) and N,N-dimethylaniline (DMA).

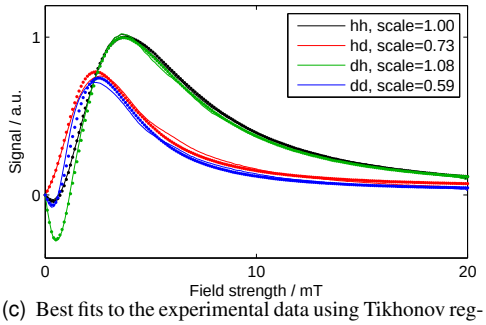

(c) Best fits to the experimental data using Tikhonov regularisation applied to all four isotopomer data sets simultaneously in order to produce a single re-encounter probability $f(t)$. The experimental data were multiplied by optimised values of "scale" before using Tikhonov regularisation. Notice that the fit is exemplary, except for small deviations in the **dd** isotopomer curve. This figure complements curve C in subfigure (d).

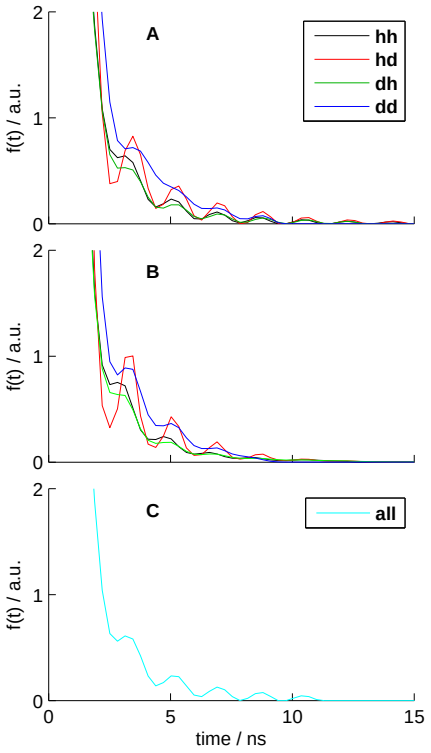

(d) Best recovered $f(t)$ for: (A) Tikhonov regularisation; and (B) maximum entropy regularisation for each of the four isotopomer combinations. (C) Tikhonov regularisation recovery of a single $f(t)$ to fit all four isotopomer combinations simultaneously.

Figure 3: Regularisation methods allow details of the diffusive motion of RPs to be recovered from experimental MFE data[11].

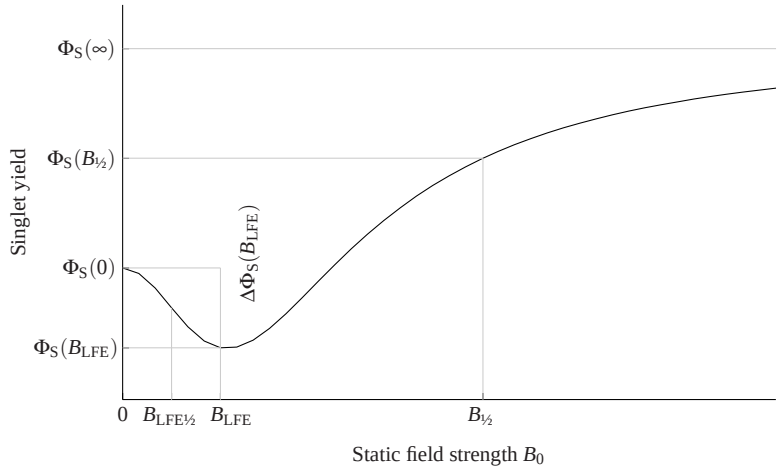

(a) MARY spectrum for a one-proton radical pair marked with the principal empirical parameters discussed in the thesis.

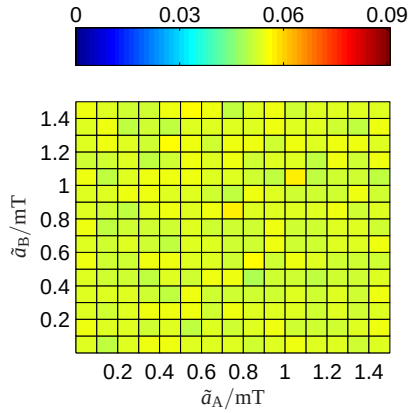

(b) Mean LFE depth $\Delta\Phi_S(B_{LFE})$ when $k = 0.01\,\mathrm{s}^{-1}$. Values range between 0.05 and 0.06.

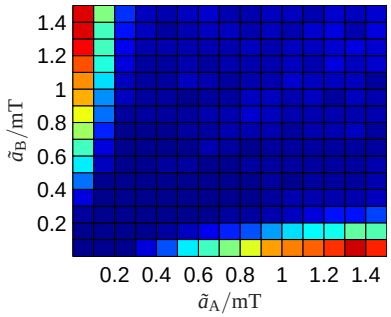

(c) Mean LFE depth $\Delta\Phi_S(B_{LFE})$ when $k = 3 \times 10^7\,\mathrm{s}^{-1}$. Values range between 0.00 and 0.08.

Figure 4: Characterising MARY spectra. Bottom: LFE depth $\Delta\Phi_S(B_{LFE})$ determined by Monte Carlo calculations in an ensemble of 12 737 radical pairs. The colour of each rectangle summarises the results from those members of the ensemble having effective HFCs which fall within it. Rate constants k were selected to be less than and comparable to the effective HFCs.

It is impossible to simulate such spectra using standard methods. Instead, I adapted an algorithm (γ–COMPUTE) from solid state NMR to successfully interpret these experiments.

I show that γ–COMPUTE simulates accurately linearly and circularly polarised RF effects.

Finally, at high RF field strengths, MFE spectra sometimes invert dramatically. I could attribute this to a "spin locking" process, shown in Figure 6. The onset of spin locking is extremely sensitive to RF field strength, which can therefore be determined from the spectra. This provides a means of calibrating the RF field coils used.

5 Magnetoreception

To avoid winter, European robins from Scandinavia and Russia migrate annually to western Europe. Robins were shown to use the Earth's magnetic field for navigation[19,20]. The mechanism beneath this compass sense is a subject of intense research. Ritz proposed that a photochemical, RPM reaction in the retina is involved, as in Figure 7. However, many questions remain unanswered — not least the identity and location of the radicals responsible. The second half of my thesis makes an important contribution to this debate.

5.1 Theory and modelling

I perform an extensive series of calculations elucidating properties necessary to produce an effective compass from realistic multinuclear radicals. I focus in particular on cryptochromes and photolyases, which are the most promising contenders to be the avian magnetoreceptor.

I introduce a new quantitative method for analysis of anisotropic MFE calculations. Decomposing the singlet yield in terms of spherical harmonics enables trends to be elucidated and presented clearly. I derived algorithms to calculate these decompositions directly or via perturbation theory. This paves the way to finding further "rules of thumb" for anisotropic magnetic field effects.

5.2 Animal experiments

Theory suggests that exposure to RF fields in addition to the Earth's magnetic field might temporarily disrupt a bird's compass sense. Subsequent behavioural experiments confirmed this prediction: for certain frequencies, strikingly weak RF fields disrupt a bird's magnetic sense[22,23].

I consider the ramifications of these data and fresh results obtained by our collaborators, shown in Figure 9. I discovered that static and RF fields of comparable strength produce comparable changes in product yield except when the RF field is at a resonant frequency. I assess whether such resonant effects may be expected in general. Figure 10 shows the results of a lengthy calculation modelling the avian magnetoreceptor as a RP like that in photolyase. Surprisingly, we conclude that only RPs where one radical has a magnetically isolated spin would show the resonant effects seen in birds.

5.3 Physico-chemical proof of principle

My colleagues in Oxford have made MFE measurements on a specially-designed CPC_{60} triad molecule (see Figure 8). This molecule shows, for the first time ever, an MFE from an Earth-strength (40 μT) field. Samples frozen in an oriented liquid crystal, have a MFE that is anisotropic. I have applied the theoretical toolkit developed in this thesis to give an interpretation of these results, which have been accepted for publication by Nature[25].

```
[ texWordCount.pl counts 1181 words excluding figures and title ]
```

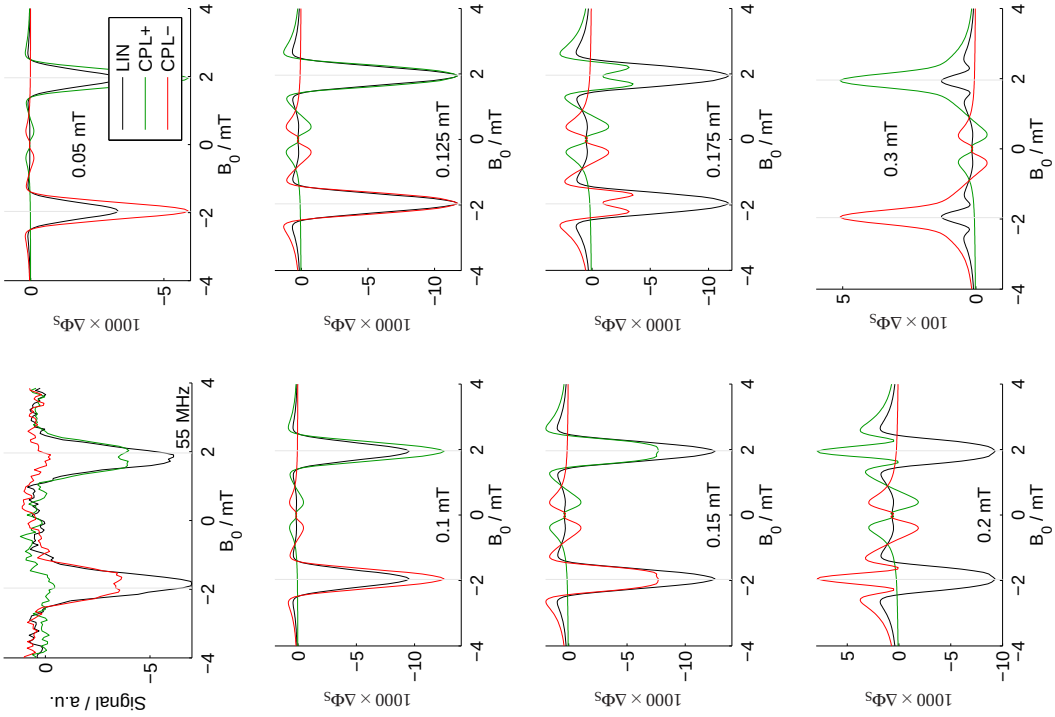

Figure 6: Spin locking effects provide a means of calibrating RF field strength. Top left: Experimental MARY-ν spectra measured in the $[\text{Py-d}_{10}^{+}\ \text{1,4-DCB}^{\bullet-}]$ radical pair at $\nu_{\text{rf}} = 55\,\text{MHz}$. Other figures: Simulations made with γ-COMPUTE or the RFT. Parameters: RMS RF field strength B_1 is marked on each figure, HFCs of $4 \times 0.083\,\text{mT}$ (^{2}D) on Py-$\text{d}_{10}^{\bullet+}$; and $2 \times 0.181\,\text{mT}$ (^{14}N) on 1,4-DCB$^{\bullet-}$, $k = 3 \times 10^7\,\text{s}^{-1}$, $n = 64$, $\theta = \pi/2$ and $\nu_{\text{rf}} = 55\,\text{MHz}$. Grey vertical lines show the Zeeman resonance static field.

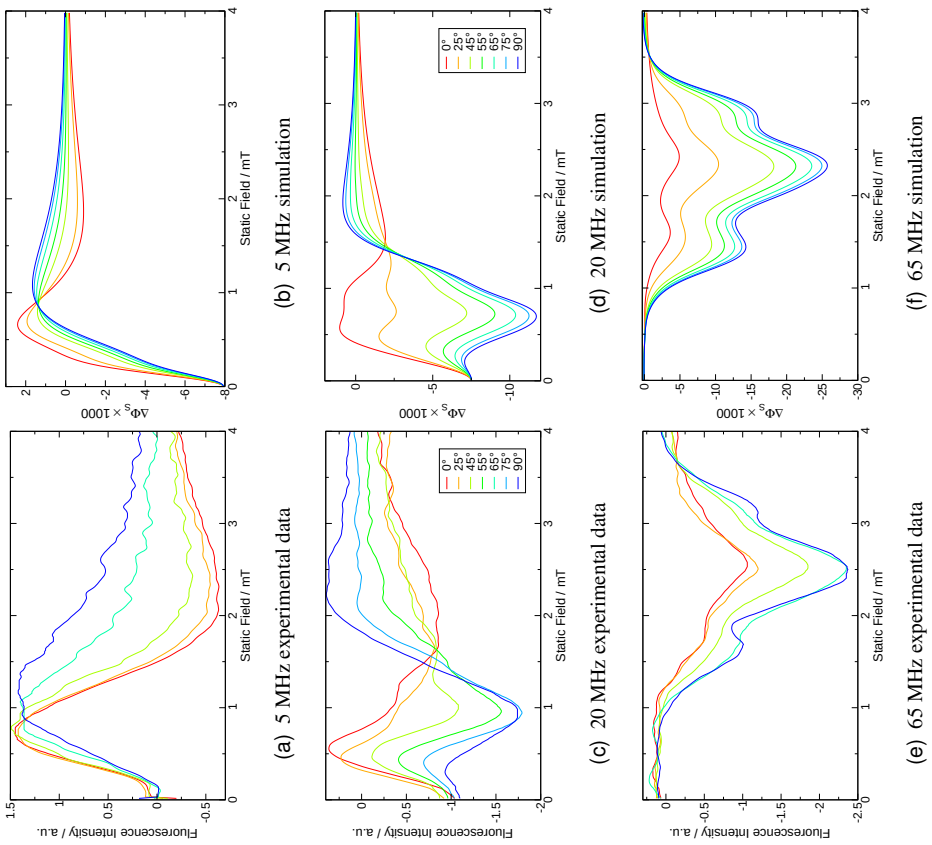

Figure 5: Experimental (left) and simulated (right) low-field optically detected EPR spectra of $[\text{Py-d}_{10}^{+}\ \text{1,3-DCB}^{\bullet-}]$ at radio frequencies of $\nu_{\text{rf}} = 5\,\text{MHz}$ (top), 20MHz (centre) and 65MHz (bottom). Values of θ are as indicated in the legend. The same colours are used for all plots, even though experimental data were not collected for some combinations of ν_{rf} and θ. The simulations were performed using $B_1 = 0.3\,\text{mT}$ and $k = 4 \times 10^7\,\text{s}^{-1}$. The experimental spectra represent the changes in the exciplex fluorescence produced by the radio frequency field.

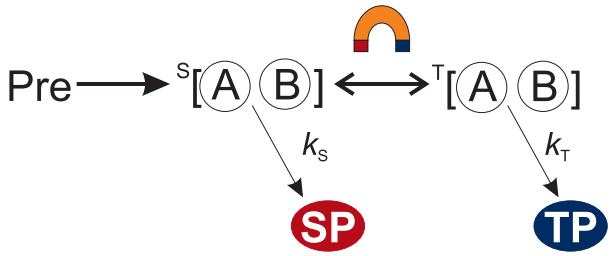

(a) Schematic of the RPM in a solid state system. A diamagnetic precursor molecule (Pre) reacts to form a spin correlated radical pair $[A^{\bullet}\ B^{\bullet}]$ in an initial singlet (S) state. Singlet–triplet interconversion is driven by magnetic interactions. The RPs react to form distinct singlet (SP) and triplet (TP) products at rates k_S and k_T respectively.

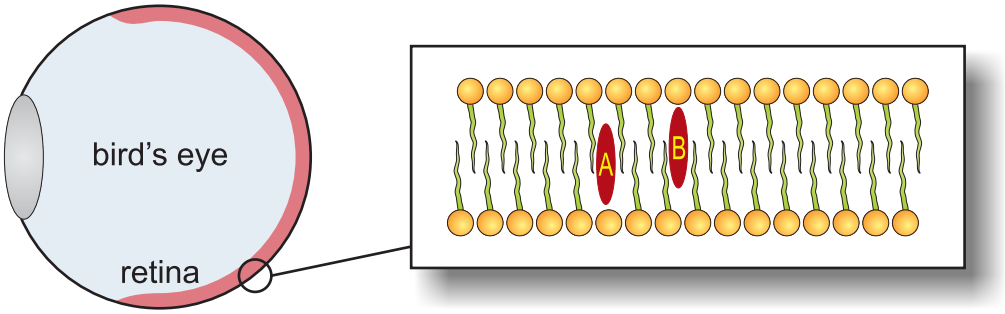

(b) Oriented radical pairs $[A^{\bullet}\ B^{\bullet}]$ could be created photochemically in the retina. The "tadpoles" represent an oriented lipid bilayer, such as that found in a membrane.

Figure 7: Schulten proposed that avian magnetoreception functions by virtue of a photochemical reaction between oriented radical pairs in the retina[21].

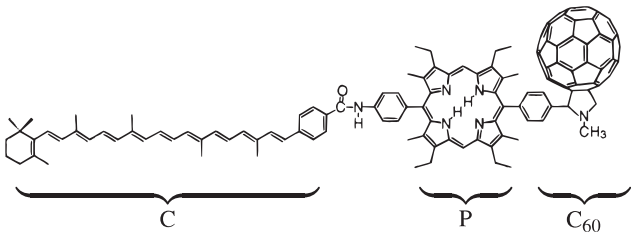

Figure 8: Carotenoid-porphyrin-fullerene model compound CPC_{60}.

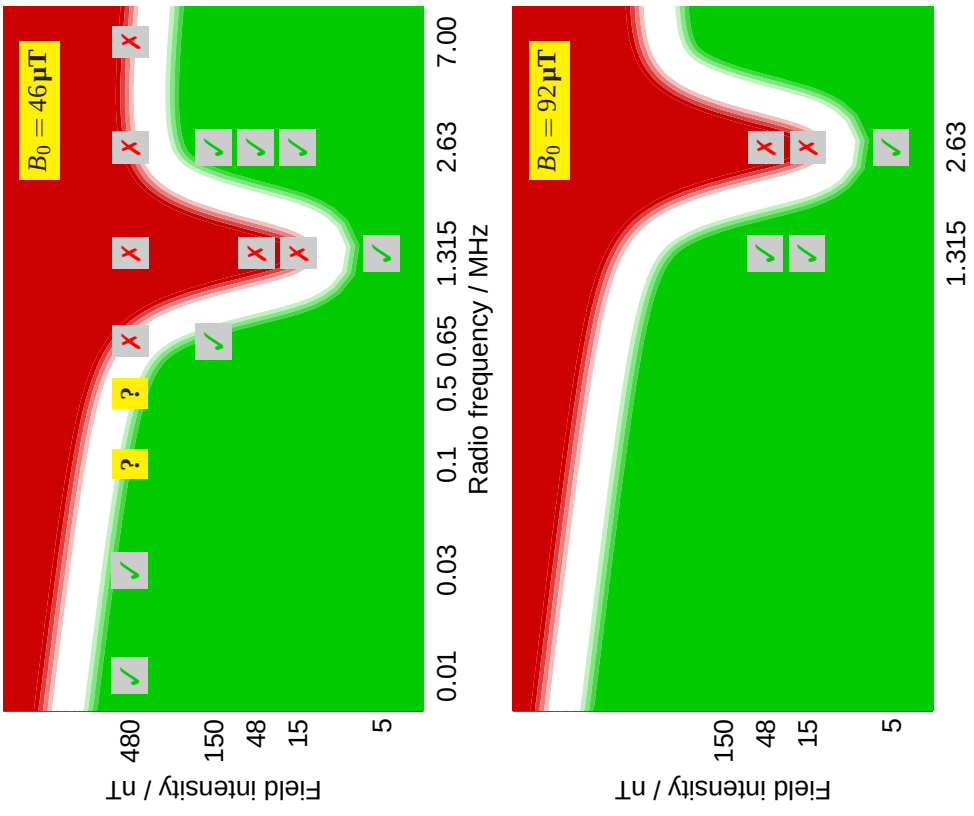

Figure 9: Summary of recent RF field effect studies on European robins[24]. Measurements were made in Frankfurt ($B_0 = 46\,\mu T$) with a vertical RF field (*i.e.* at an angle of 24° relative to the geomagnetic field). Green ticks denote successful seasonally-appropriate orientation; red crosses denote disorientation; question marks denote biaxial distributions where some subjects headed in the seasonally-appropriate direction whilst others headed in the opposite direction.

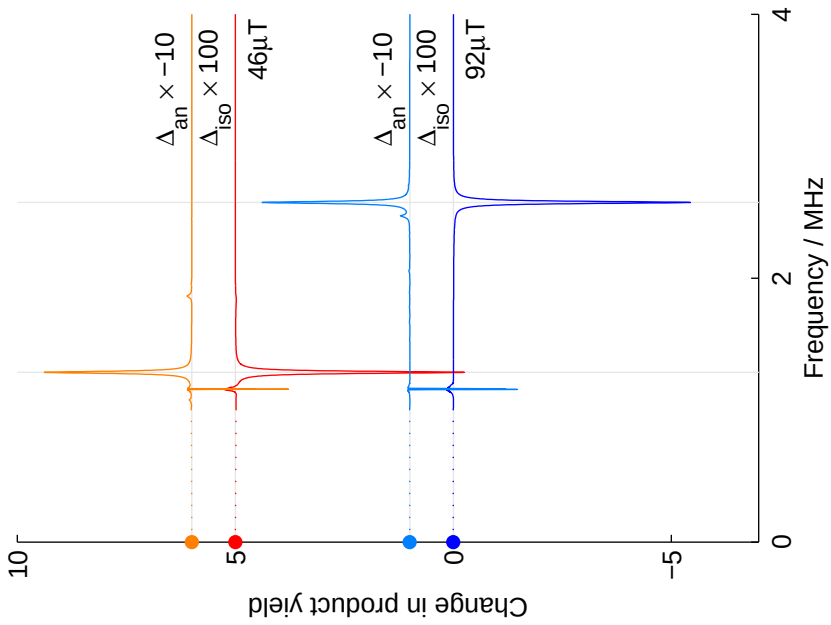

Figure 10: Calculated radiofrequency MFEs for a RP comprising N5, N10 and H5 from FADH$^\bullet$ in static fields $B_0 = 46$ and $92\,\mu T$. The corresponding Zeeman frequencies are marked with vertical grey lines. Hyperfine tensors and the atom numbering for FADH$^\bullet$ are given in the thesis. Other parameters: $\varepsilon_0 = 24^\circ$, $\varepsilon_1 = 0^\circ$, $k = 5 \times 10^4\,s^{-1}$, $B_1 = 1\,\mu T$ and $n = 64$. As far as possible these values were chosen to match those in recent experiments on European robins[24]. For clarity, the curves are offset vertically by 0, 1, 5 or 6 units.

References

[1] Christopher T. Rodgers. *Magnetic Field Effects in Chemical Systems*. D.Phil. thesis, University of Oxford, 2007.

[2] U.E. Steiner and T. Ulrich. *Chem. Rev.*, 89:51–147, 1989.

[3] H. Hayashi. *Introduction to Dynamic Spin Chemistry*, volume 8. World Scientific, 2004.

[4] R. Kaptein and J.L. Oosterhoff. *Chem. Phys. Lett.*, 4(4):195–197, 1969.

[5] G.L. Closs. *JACS*, 91(16):4552–4554, 1969.

[6] K.A. McLauchlan and U.E. Steiner. *Mol. Phys.*, 73:241–263, 1991.

[7] B. Brocklehurst and K.A. McLauchlan. *Int. J. Rad. Biol.*, 69(1):3–24, January 1996.

[8] F.J. Adrian. *J. Chem. Phys.*, 54(9):3912–3917, 1971.

[9] F.J. Adrian. *J. Chem. Phys.*, 54(9):3918–3923, 1971.

[10] F.J. Adrian. In *Chemically Induced Magnetic Polarization*, volume 34 of *NATO Advanced Study Institute: Series C*, pages 77–105. D. Reidel Publishing Company, 1977.

[11] Christopher T. Rodgers, S.A. Norman, K.B. Henbest, C.R. Timmel, and P.J. Hore. Determination of radical re-encounter probability distributions from magnetic field effects on reaction yields. *JACS*, 129(21):6746–6755, 2007.

[12] D.V. Stass, N.N. Lukzen, B.M. Tadjikov, and Yu.N. Molin. *Chem. Phys. Lett.*, 233(4):444–450, 1995.

[13] D.V. Stass. Personal communication. "Re: Low Field Effect", 2006.

[14] C.R. Timmel, U. Till, B. Brocklehurst, K.A. McLauchlan, and P.J. Hore. *Mol. Phys.*, 95(1):71–89, 1998.

[15] K. Schulten and P.G. Wolynes. *J. Chem. Phys.*, 68(7):3292–3297, 1978.

[16] Christopher T. Rodgers, K.B. Henbest, P. Kukura, C.R. Timmel, and P.J. Hore. Low-field optically detected EPR spectroscopy of transient photoinduced radical pairs. *J. Phys. Chem.*, 109A:5035–5041, 2005.

[17] K.B. Henbest, P. Kukura, Christopher T. Rodgers, P.J. Hore, and C.R. Timmel. Radio frequency magnetic field effects on a radical recombination reaction: A diagnostic test for the radical pair mechanism. *JACS*, 126(26):8102–8103, 2004.

[18] C.R. Timmel and K.B. Henbest. *Phil. Trans. Roy. Soc. London A*, 362:2573–2589, 2004.

[19] W. Wiltschko and F.W. Merkel. *Verh. dt. zool. Ges.*, 59:362–367, 1966.

[20] W. Wiltschko and R. Wiltschko. *Science*, 176(4030):62–64, 1972.

[21] K. Schulten, C.E. Swenberg, and A. Weller. *Zeitschrift fuer Physikalische Chemie Neue Folge*, 111:1–5, 1978.

[22] T. Ritz, P. Thalau, J.B. Phillips, R. Wiltschko, and W. Wiltschko. *Nature*, 429:177–180, 2004.

[23] P. Thalau, T. Ritz, K. Stapput, R. Wiltschko, and W. Wiltschko. *Naturwissenschaften*, 92(2):86–90, 2005.

[24] T. Ritz, R. Wiltschko, Christopher T. Rodgers P.J. Hore, K. Stapput, P. Thalau, C.R. Timmel, and W. Wiltschko. Magnetic compass of birds is based on a molecule with optimal directional sensitivity. *In peer review at Nature*, 2008.

[25] Kiminori Maeda, Kevin B. Henbest, Filippo Cintolesi, Ilya Kuprov, Christopher T. Rodgers, Paul A. Liddell, Devens Gust, Christiane R. Timmel, and P. J. Hore. Chemical compass model of avian magnetoreception. *Nature*, 2008 (Accepted, in press).